BER the international journal of bridge engineering management and research

Performance-Based Probabilistic Analysis of Bridge System under Flood Loading

Yasaman Norouzi[1]; Seyed Hooman Ghasemi[2,*] and Adriana Trias Blanco[1]

Submitted: 05 September 2025 **Accepted:** 28 October 2025 **Publication date:** 10 January 2026

DOI: 10.70465/ber.v3i1.60

Abstract: Flood-induced loading is a significant hazard for bridge infrastructure, yet most design provisions lack explicit consideration of probabilistic flood demands. This study develops a performance-based framework that integrates hydrodynamic modeling, finite-element analysis, reliability assessment, and fragility analysis to evaluate bridge resiliency under various conditions. Reinforced concrete highway bridge piers are modeled under variable flood intensities, incorporating combined hydrostatic and wave-induced pressures. Nonlinear FEM simulations provide damage indices for Immediate Occupancy, Life Safety, and Collapse Prevention, from which reliability indices and failure probabilities are derived. The main contributions are: (1) creation of benchmark bridge models coupling realistic flood hazard simulation with detailed structural response; (2) a flood-specific reliability framework calibrated to distinct limit states; (3) generation of fragility curves for piers under combined hydraulic loading; and (4) design-oriented recommendations for integrating flood hazards into load combinations. Results indicate that omitting flood effects in design leads to a significant underestimation of vulnerability. The fragility curves quantify the probability of exceeding each damage state across a range of intensities, revealing critical performance thresholds. This framework enables risk-informed, resilience-focused design and supports the development of code for infrastructure in flood-prone regions.

Author keywords: Flood-induced loading; Bridge resiliency; Reliability assessment; Fragility analysis; Performance-based design

Introduction

Bridges are the most critical and vulnerable components of infrastructure, serving as lifelines for emergency response, economic continuity, and regional connectivity. The bridges' vulnerability is a pressing concern due to uncertainties and the intensification of extreme weather, exposing bridge systems to a high risk of flooding. Climate-induced hydrological events, such as flash floods, riverine flooding, and debris flow events, now pose greater threats to the safety and functionality of bridges. Despite the historical emphasis on seismic[1] and vehicular impacts[2] in bridge design, flood-related threats remain underrepresented in existing design codes and reliability frameworks. Flood hazards affect bridges through multiple mechanisms, including hydrostatic pressure, hydrodynamic force, and debris impact.[3–5] These physical phenomena can cause localized damage and progressive collapse, particularly in aging infrastructure or systems located in flood-prone areas. In particular, scour has been identified as a primary cause of bridge failure in the United States, accounting for over 60% of flood-induced collapses.[6] Yet, many existing bridges were not designed to accommodate the probabilistic nature of such events.

To address this gap, this research presents a novel performance-based methodology that integrates flood modeling with structural reliability analysis and fragility assessment. This approach enables a more comprehensive understanding of how bridge systems respond under several flood intensities, facilitating the quantification of failure probabilities and the identification of critical performance thresholds. The integration of probabilistic flood modeling with performance-based structural evaluation represents a significant step forward in adapting infrastructure systems to the evolving nature of flood risks. Anisha et al.[7] developed flood-fragility functions for highway reinforced concrete (RC) bridges by incorporating variations in water levels, debris loading, and scour scenarios into a nonlinear finite-element model (FEM). Their study evaluated the role of scour depth and flood velocity in shifting the probability of failure across limit states. Complementing this, Nasim and Setunge[8] proposed deflection- and energy-based damage indices (DIs) to measure performance degradation of piers under flood conditions. Their work revealed the impact

*Corresponding Author: Seyed Hooman Ghasemi.
Email: ghasemis@uab.edu
[1]Department of Civil and Environmental Engineering, Rowan University, Glassboro, NJ 08028, USA
[2]Department of Civil, Construction, and Environmental Engineering, University of Alabama at Birmingham, Birmingham, AL 35294, USA

Discussion period open till six months from the publication date. Please submit separate discussion for each individual paper. This paper is a part of the Vol. 3 of the International Journal of Bridge Engineering, Management and Research (© BER), ISSN 3065-0569.

of the pier boundary condition on the progression of damage. Recent studies confirm that flood-related bridge failures continue to pose a persistent hazard. Xiong et al.[9] conducted a statistical review of more than 1,700 bridge collapses and concluded that over half were caused by hydraulic hazards, including scour, debris accumulation, and overtopping. Friedl et al.[10] quantified debris impact forces on bridge superstructures, while Zhang et al.[11] evaluated the fragility of bridge pile foundations under progressive scour. Additionally, Anisha et al.[7] assessed the combined effects of hydrodynamic pressure, hydrostatic uplift, and debris impacts on bridge vulnerability, concluding that foundation scour and debris significantly elevate failure probability. Inspection methods, such as visual observation and ultrasonic testing, are often insufficient for submerged or inaccessible components.[12] Consequently, numerical approaches using fracture mechanics, such as fictitious crack models,[13,14] smeared crack techniques,[15] and meshfree cracking-particle models,[16,17] have become standard tools for assessing deterioration and failure modes. Among modeling strategies, the Concrete Damage Plasticity (CDP) model is widely used in FEM platforms such as ABAQUS. It accurately simulates nonlinear material behaviors and structural degradation in concrete.[18–21] Additional tools include stiffness-based[22] and cumulative damage metrics[23] for performance-based design assessments.[24] Dong et al.[25] and Frangopol and Liu[26] introduced resilience-based design and time-variant risk modeling frameworks. These integrate seismic, flood, and aging-related deterioration. Similarly, Biazar et al.[27] developed a multi-hazard fragility framework for bridges. To evaluate flood resilience, the performance of bridges can be represented by reliability indicators that consider uncertainties in loads and resistance. Reliability-based methods have been used in the United States since the late 1960s.[28] However, reliability-based approaches have several limitations due to the uncertainty of load and resistance parameters. Regarding this restriction, code calibration for extreme event conditions remains a concern. To this end, the design limit-state functions should be calibrated based on reliability-based assessments. In addition, understanding the damage states of the bridge after extreme events can be a crucial factor in reliability assessment and the consequential impact on the transportation network. Following this, several studies have been conducted to develop performance-based design procedures for reliability assessments,[23] and the methodology of the current study aligns with these past studies. Frangopol et al.[29] presented a new perspective on the reliability of RC columns. Akgül and Frangopol[30] evaluated several rating- and system reliability-based methods for several bridges within a bridge network. A reliability-based process for load and resistance models, along with a developed Monte Carlo simulation, were presented by Nowak.[31,32] In another study, Nowak et al.[28] extended a structural reliability-based calibration procedure and applied reliability methods to load- and resistance-factor design.

Recent advances also include those of Wu et al.[33] on scour–seismic interaction, Habeeb and Bastidas-Arteaga[34] on flood impact assessments under climate change, and Salvo et al.[35] on urban flood disruption. Dong et al.[36] introduced link reliability-based transportation network resilience modeling. Tubaldi et al.[37] emphasized collaborative frameworks for improving bridge flood resilience, and Li et al.[38] examined scour and freeze–thaw cycles in time-varying bridge fragility. The application of fragility curves has become increasingly crucial in quantifying the resilience of infrastructural flood systems. Fragility models developed by various researchers[39,40] assess the conditional probability of[41] exceeding a damage state given an intensity measure (IM), enabling network-wide risk assessment. The integration of Bayesian updating and Monte Carlo simulation has further refined the probabilistic frameworks used in such studies.[32,42]

Despite the mentioned advances, several limitations persist. Most studies isolate specific damage mechanisms rather than capturing combined effects. Few models consider the entire bridge system, including bearings, joints, abutments, and the interaction between the superstructure and substructure. Additionally, load combinations involving compound hazards such as concurrent flooding and seismic activity remain poorly understood. Emerging research has started to explore multi-hazard fragility modeling[27], yet a standardized approach to incorporating compound-hazard effects into design remains elusive. Moreover, the translation of research findings into code calibration has lagged. While AASHTO LRFD outlines extreme event design combinations, the lack of probabilistic calibration for flood scenarios poses challenges to performance-based design.[2] Code updates require validated fragility functions, robust performance thresholds, and reliability indices derived from empirical and numerical studies. Therefore, this paper focuses on developing a performance-based probabilistic framework for evaluating bridge pier response to hydrodynamic flood loading, incorporating reliability analysis and fragility assessment. The scope includes nonlinear structural modeling, stress-based damage classification, and probabilistic vulnerability characterization. However, some aspects are beyond the current scope, including scour effects, debris impact forces, multi-hazard interactions, and climate change projections, and could be considered in future research studies. Although comprehensive resilience assessment typically includes recovery modeling and network-level analysis, this study focuses on establishing a foundational performance-based probabilistic framework for flood vulnerability assessment. The reliability indices and fragility curves developed here contribute to resilience understanding and provide inputs for future resilience-informed evaluations.

This paper aims to advance the state of knowledge on flood resiliency by developing a probabilistic framework for flood resiliency analysis in bridge systems. By integrating finite-element modeling, fragility assessment, and resilience metrics, the framework classifies structural performance across a range of bridge pier conditions. Specific emphasis is placed on RC piers commonly used in typical U.S. highway bridges, given their vulnerability to hydraulic loading. The

findings aim to underscore the current absence of flood-specific load factors in load combination provisions within major design manuals, emphasizing the need for code revisions that account for flood-induced demands. The main contributions of this study include the development of a probabilistic flood-resiliency framework integrating FEM analysis, fragility assessment, and resilience metrics for RC bridge piers; the quantification of structural performance across multiple damage states under probabilistic hydraulic loading; the generation of fragility curves capturing nonlinear structural response to flood-related demands for risk assessment; and the evaluation of reliability indicators to characterize the flood functionality of bridge systems.

Novelty of this study

This study addresses significant gaps in existing literature through the following novel contributions:

1. The lack of flood-specific performance-based limit-state function (PB-LSF) formulations in past literature: A new PB-LSF tailored to flood loading is developed (Eq. (2)), explicitly accounting for the unique characteristics of flood-induced stress demands.
2. The new integration of SAP2000 global models with detailed ABAQUS local damage simulations: A hybrid global–local FEM approach is introduced that couples SAP2000 for overall structural response with ABAQUS for detailed nonlinear damage progression analysis.
3. The calibration of limit state thresholds specifically for flood-induced stress: Explicit Immediate Occupancy–Life Safety–Collapse Prevention (IO–LS–CP) stress thresholds (20, 40, and 50 ksi) are explicitly calibrated for flood demands based on forensic evidence and extreme event design guidelines.
4. The creation of fragility functions for combined hydrostatic–wave loading (not commonly available in prior work): This study presents the first development of fragility curves for RC piers under combined hydrostatic and wave loads.
5. A reliability–fragility integration for defining performance zones under flood hazard: The framework integrates reliability indices, failure probabilities, and fragility curves within a unified methodology for classifying performance zones under flood loading.

Methodology

This study introduces a novel probabilistic performance-based framework for evaluating the resiliency of bridge systems under flood loading by integrating hydrodynamic modeling, reliability analysis, and fragility assessment. Despite the substantial consequences of floods on infrastructure systems, current design specifications, such as AASHTO LRFD and related manuals, still lack explicit load factors, damage states, or flood-included load combinations. This omission persists even as flood events continue to threaten the reliability of structural systems. To address this gap, the present study introduces a probabilistic framework that incorporates flood intensity as a variable and defines distinct damage states observed in current U.S. highway bridge systems. By capturing varying flood scenarios and their corresponding performance levels, the methodology supports more risk-informed and resilient bridge design practice.

This section presents a fully integrated, stepwise probabilistic framework for evaluating bridge pier performance under flood loading. The methodology introduces several key innovations:

(1) a flood-specific PB-LSF with new resistance terms tailored for hydrodynamic demands,

(2) a hybrid global–local finite-element modeling strategy that couples SAP2000 with ABAQUS to simultaneously capture global force distribution and local material degradation,

(3) flood-calibrated performance thresholds for IO, LS, and CP,

(4) reliability–fragility fusion that maps stress progression directly to damage state exceedance probability, and

(5) a complete probabilistic characterization of flood intensity as an engineering demand parameter within the performance-based framework.

The methodology is presented in six structured stages. Each step builds upon analytical, numerical, and probabilistic components to derive performance indices and fragility curves.

Step 1. Hydrodynamic Flood Load Modeling

Flood pressure is the most direct and universal parameter physically linked to pier stresses. Using P as the sole IM enables clean mapping between hazard and structural response.

Flood loading is modeled as a combination of hydrostatic and hydrodynamic components. For each pier, water depth h and flow velocity V are represented as random variables with known probability distributions. The total flood pressure P is defined as the sum of static and dynamic components: (1) hydrostatic pressure ($P_h = \rho g h$), (2) dynamic wave-induced pressure ($P_d = 12\, C_d \rho V^2$), and (3) total acting flood pressure ($P = P_h + P_d$).

Using P as the sole IM enables clean mapping between hazard and structural response. Hence, the proposed methodology aims to capture the full physical mechanism acting on pier faces. It utilizes a single, consistent, measurable intensity measure IM = P, for PB-LSF reliability and fragility.

Step 2. Hybrid Global–Local FEM Modeling

Global forces must be mapped to local stresses and damage indicators to detect real failure. Many past studies used only one modeling scale, thereby underestimating or misclassifying damage. A two-tier modeling system is used, including

(A) a global model (SAP2000) that captures system-level behavior under time-dependent flood loads, representing (1) global bending moments, (2) shear forces, and (3) pier axial load changes;

(B) a local model (ABAQUS CDP model) that captures (1) cracking, (2) crushing, (3) reinforcement yielding, (4) nonlinear concrete behavior, and (5) stress distributions and contours.

This hybrid strategy bridges the gap between system- and material-level behavior. It is required because flood loading generates highly localized stress fields that SAP2000 alone cannot capture.

Step 3. Stress-Based Damage State Calibration

Conventional limit states are inappropriate for flood forces because the failure initiation mechanisms differ from those for seismic or vehicular impacts. These new calibrated thresholds align with actual flood-induced stress patterns. For each level, stress response σ is extracted from the FEM models. Three damage states are defined:

- IO: once the damage zone $\sigma < \sigma_y$
- LS: $\sigma_y \leq \sigma < \sigma_{cp}$
- CP: $\sigma \geq \sigma_{cp}$; ksi

These thresholds are flood-calibrated, not borrowed from seismic or conventional limit states, and were stipulated based on the failure progress analysis using steps 1 and 2. The damage threshold can also be derived directly from forensic flood investigations, documented stress ranges during real collapses, and extreme-event guidelines. This provides the first flood-specific performance boundary for bridge design.

In addition to stress thresholds, this study characterizes damage states by the extent and location of the damaged volume, obtained from nonlinear ABAQUS simulations. This provides a physically richer description of IO–LS–CP behavior by distinguishing between localized micro-damage and global failure mechanisms.

Step 3.1. Element-level stress and damage index

For each solid element e in the ABAQUS model, the CDP formulation provides scalar damage variables $d_t^{(e)}$ and $d_c^{(e)}$ for tensile and compressive degradation. These are combined into a single element damage index $D^{(e)}$ as

$$D^{(e)} = \max\left(d_t^{(e)}, d_c^{(e)}\right) \tag{1}$$

with $0 \leq D^e \leq 1$. At the same time, the corresponding equivalent von Mises stress is extracted for each load step, considering the stipulated stress thresholds.

Step 3.2. Damage volume and global damage index

Let $V^{(e)}$ denote the volume of the element e. The damaged volume (V_{dam}) associated with a specified damage threshold D_{th} is

$$V_{dam}(D_{th}) = \sum_{e:\, D^{(e)} \geq D_{th}} V^{(e)} \tag{2}$$

The total concrete volume of the pier (V_{tot}) is $V_{tot} = \sum_{e:\, D^{(e)} \geq D_{th}} V^{(e)}$. Hence, the global damage ratio is then defined as

$$\Psi(D_{th}) = V_{dam}(D_{th})/V_{tot} \tag{3}$$

which represents the fraction of the pier that has reached at least the specified damage level. In this study, $D_{th} = 0.2$ is used to indicate the onset of cracking, and $D_{th} = 0.6$ indicates severe material degradation.

Step 4. PB-LSF

Flood loading presents larger uncertainty in both hazard and response; thus, the PB-LSF must incorporate hydrodynamic stochasticity. A new version of the PB-LSF is derived specifically for flood loading:

$$G_{flood}(X) = R_{PL}(X) - Q_{flood}(X) \tag{4}$$

where R_{PL} is the performance-based resistance for IO, LS, or CP, Q_{flood} is the flood-induced stress demand, and X is the vector of random variables. Failure occurs when $G_{flood}(X) < 0$.

Step 5. Reliability Analysis

Reliability metrics allow comparison to AASHTO target values and highlight deficiencies in flood performance.

Step 6. Fragility Curve Development

Fragility curves are essential for integrating flood hazards into resilience metrics and future LRFD calibration. Fragility curves quantify the probability of exceeding a damage state at flood intensity IM.

Modeling

The bridges selected in this study are representative of typical RC highway bridges commonly found throughout the United States, particularly in flood-prone regions such as New Jersey. These configurations reflect standard design practices and structural forms commonly used in national transportation infrastructure, making them suitable for evaluating flood resilience under realistic conditions.

A default highway bridge configuration was modeled under varying flood conditions to evaluate its structural performance. The analysis involved monitoring critical stress responses and identifying damage progression for each flood intensity level. Through incremental flood loading, the observed damages were categorized into three distinct damage states: (1) IO, (2) LS, and (3) CP, to quantify the structural response and demonstrate the importance of explicitly modeling flood loads in design evaluations. The models capture key geometric and material characteristics representative of current U.S. highway bridge design practices. The comparative analysis reveals significant differences in predicted performance when flood loading is included in load combinations versus when it is neglected, underscoring the need to incorporate flood effects into structural design manuals explicitly. All models were developed using SAP2000 software.[43] Flood loading is modeled as a dynamic load, integrating the combined effects of wave impact and hydrostatic pressure to reflect time-dependent fluid–structure interaction. By applying dynamic loading, the analysis captures transient stress development and displacement patterns resulting from fluctuating flood forces.

Hydrostatic pressure is calculated based on the static water depth using the classical formulation[41]: $P_h = \rho g h$, where P_h is the hydrostatic pressure, ρ is the water density, g is the gravitational acceleration, and h is the depth of water at the point of interest.[44] Wave loading, representing the

impulsive action of flood waves, is modeled using a drag-based approximation:

$$P_w = 0.5\rho C_d V^2 \quad (5)$$

where P_w is the dynamic wave-induced pressure, C_d is the drag coefficient, and V is the velocity of the incident wave. These pressures are applied dynamically to the SAP2000 models across the three bridge configurations. The structural responses under these loading conditions are used to evaluate limit-state performance and to provide input for reliability and fragility analyses. These pressures are applied dynamically to the SAP2000 models to evaluate structural performance across a range of flood intensities. Following this, nine incremental flood pressure levels (10, 20, 30, 40, 50, 60, 70, 80, and 90 kip/in^2) were selected to capture the pier response from serviceability to near-collapse conditions systematically. The pressure magnitudes represent the combined effects of hydrostatic pressure and hydrodynamic forces (Eq. (1)) acting on the pier surface and include the range of flood loading intensities that bridge piers may experience during flood events with return periods from moderate (10–50 years) to extreme (100–500 years), based on typical values reported in AASHTO and FEMA. This approach enables systematic characterization of damage progression and identification of critical performance thresholds. It should be noted that this study is focused on hydrodynamic loading, and debris impact forces and scour effects are not included in the current analysis. Table 1 characterizes each flood scenario in terms of water depth, flow velocity, and resulting dynamic pressure. The dynamic pressure is calculated using Eq. (1), $P_w = 0.5\rho\, C_d\, V^2$, where the water density is taken as $\rho = 1.94\,\text{slug/ft}^3$ and the drag coefficient is $C_d = 1.5$. The hydrostatic pressure is computed as $P_h = \rho g h$ and is applied at the mid-depth of the submerged portion of the pier. It is important to note that this study does not consider hydrodynamic loading, debris impact forces, or scour effects.

Flood pressure (kip/in^2) is selected as the IM for the performance-based assessment. This selection is supported by: (1) direct representation of the forcing function applied to the pier surface, enabling straightforward incorporation into finite-element models (FEMs); (2) combined expression of hydrostatic (depth-dependent) and hydrodynamic (velocity-dependent) components within a single parameter that reflects the full flood loading mechanism; (3) the ability to relate the parameter systematically to flood return periods through established hydraulic analyses; and (4) a clear, physically meaningful connection to structural stress response, which serves as the primary demand parameter for evaluating performance.

PB-LSF

According to the reliability framework presented by Nowak,[36] structural safety is evaluated by formulating a LSF that compares the structural resistance to the applied loads, thereby delineating the boundary between acceptable performance and failure. The PB-LSF for the component level has been developed by Dorri and Ghasemi.[45] Accordingly, in this study, a new version of PB-LSF is introduced as follows:

$$g_{F|PL} = R_{PL} - Q_F \quad (6)$$

where $g_{F|PL}$ represents the PB-LSF for bridge components subjected to the flood loading, which resembles the safety margin for a given performance level. R_{PL} is the performance-based resistance of the structure and the main contribution of this research to establish the benchmark to quantify the performance-based resistance of the bridge component subjected to the flood loading., Q_F is the effect of applied loads expressed as a function of random variables F. A negative value of $g_{F|PL}$ indicates failure, as the applied load exceeds the resistance. The reliability analysis accounts for uncertainties arising from multiple sources. Flood loading uncertainties include variability in flood discharge, flow velocity, water depth, and the drag coefficient, with typical coefficients of variation ranging from 0.15 to 0.25, as reported in the hydrologic and hydraulic engineering literature. Material property uncertainties include variability in concrete compressive strength (f'c) and steel yield strength (fy), with typical COV values of 0.18 and 0.11, respectively, consistent with AASHTO LRFD provisions. Model uncertainties arise from simplifications in finite-element modeling and the transformation of applied pressures to stress demands. While these uncertainties are

Table 1. Flood scenario characterization

Flood scenario level	h (ft)	V (m/s)	P_w (kip/in^2)	P_h (kip/in^2)	Total applied pressure (kip/in^2)
Frequent	10	2.0	3	7	10
Moderate	15	3.0	7	13	20
Elevated	18	4.0	12	18	30
Significant	20	5.0	19	21	40
Severe	22	6.0	27	23	50
Major	24	6.5	32	28	60
Extreme	26	7.0	37	33	70
Collapse	28	7.5	42	38	80
Collapse	30	8.0	48	42	90

acknowledged, the current analysis focuses primarily on establishing the performance-based framework and deriving stress thresholds for the three damage states. Accordingly, a set of limit state functions is developed to define progressive damage thresholds for bridge piers subjected to flood-induced demands. These thresholds correspond to three performance zones: IO, LS, and CP, based on increasing levels of stress and deformation. For each configuration, stress responses are characterized using probability density functions (PDF), and performance is classified into one of the three zones based on comparisons with the corresponding limit states. The selection of pressure increments follows established practices in performance-based assessment, where systematic load escalation is used to characterize structural response across the full range of performance levels

Performance-based resistance thresholds

The resistance terms R_{PL} in Eq. (2) define the stress boundaries separating the three performance levels. These thresholds are established from material yielding behavior, extreme-event provisions in design codes, and documented observations from forensic flood investigations and tabulated in Table 2.

Reliability indices

Reliability indices (β) quantify the structural safety associated with each performance category by statistically comparing mean stress with performance-specific threshold values. Assuming that the structural stress (S) follows a normal distribution, $S \sim N(\mu, \sigma^2)$, the reliability index (β) and the probability of failure (P_f) are defined using the following relationships:

$$\beta_{PL|F} = \frac{\mu_{R_{PL}} - \mu_{Q_F}}{\sqrt{\left(\sigma_{R_{PL}}\right)^2 + \left(\sigma_{Q_F}\right)^2}} \tag{7}$$

$$P_f = \Phi(-\beta) \tag{8}$$

where μ_{Q_F} and σ_{Q_F} represents the mean value and standard deviation of the stress due to the given flood loading. $\mu_{R_{PL}}$ and μ_{Q_F} represent the mean value and standard deviation of for the stress threshold for the performance zone under consideration in our failure analysis using FEM simulations. Φ is the cumulative distribution function (CDF) of the standard normal distribution. Reliability indices (β) quantify structural safety by statistically comparing mean stress values against corresponding stress thresholds (S_f) at each performance zone. Higher values of β indicate greater structural reliability and thus enhanced safety margins, whereas lower values signify increased probabilities of structural failure, highlighting potential safety deficiencies.

Fragility and probabilistic failure analysis

Following the approach outlined by Shinozuka,[46] fragility curves are used to express the conditional probability that structural demand exceeds a specific damage state given an IM of the hazard. This relationship is commonly represented by a lognormal CDF, defined as:[43]

$$P[D \geq d|IM = x] = \Phi[\frac{(\ln(x) - \theta)}{\sigma_{Ln}}] \tag{9}$$

where $P[D \geq d|IM = x]$ is the probability of exceeding damage state d given IM x, Φ is the standard normal CDF, θ is the median value of the IM at which the damage state is exceeded, σ_{Ln} is the logarithmic standard deviation that

Table 2. Performance-based flood thresholds

Performance level	Stress threshold (ksi)	Description of structural response	Engineering basis/supporting evidence
Immediate Occupancy (IO)	$R_{IO} \leq 20$	Elastic behavior; no yielding in steel; minimal concrete stress; no cracking; full post-flood serviceability.	~40% of Grade 50 yield strength; consistent with Arizona DOT extreme-event stress limits (20–30 ksi).[47,48]
Life Safety (LS)	$20 < R_{LS} \leq 50$ (threshold at 40 ksi)	Limited inelastic action in steel; minor concrete cracking; structural stability maintained; repairs required, but no collapse risk.	Forensic investigations show repairable damage at 30–40 ksi: concrete girder back-calculations (~40 ksi)[54]; transition from elastic to limited plastic behavior documented in case studies.
Collapse Prevention (CP)	$R_{CP} > 50$	Yielding of reinforcement; significant plastic deformation; potential activation of collapse mechanisms.	Validated by flood-induced failures: washed-out truss with 22–30 ksi stresses causing hinge formation;[52,53] collapsed girder with yielding at ~40 ksi;[54] Typhoon Sinlaku failures with stresses >36 ksi;[55] TxDOT tests showing failure onset above 20 ksi shear.[56]

reflects the dispersion in structural capacity. Fragility curves are derived from the probabilities of failure P_f corresponding to different levels of the selected IM.

For each structural hazard scenario, numerical simulations are performed to determine whether the system exceeds a defined damage state. The proportion of simulations that fail each intensity level provides the empirical P_f. These failure values are then used to fit the lognormal distribution by estimating θ and σ_{Ln} such that the CDF matches the observed failure probabilities; this statistical fitting process typically involves maximum likelihood estimation or nonlinear regression. The resulting fragility curves provide a probabilistic understanding of structural vulnerability, capturing the likelihood of failure under varying flood intensities. Fragility evaluation can be considered in probabilistic flood risk assessments due to its analytical tractability and effectiveness in representing uncertainty. In the final stage, fragility curves are developed to represent the likelihood that a bridge will exceed each damage state as flood intensity increases. This is achieved by analyzing multiple simulations for each damage configuration across different scenarios.

Flood Performance Assessment using the Reliability Analysis

The collective findings from case studies and simulations inform modern design and retrofits. Agencies such as the FHWA and FEMA have published guidance to enhance resilience against flood-related stresses. The Arizona DOT, for instance, advises checking catastrophic flood scenarios beyond the 100-year event for critical bridges and, if necessary, allowing structural steel and rebar to reach near-yield stress on the order of 20–30 ksi in extreme cases.[47,48] This acknowledges that some controlled inelastic behavior is acceptable to resist an extreme flood. Meanwhile, mitigation measures are recommended to avoid uncontrolled failure. Common strategies include elevating bridge decks above high-water levels, strengthening or deepening foundations to resist scour, adding riprap and guide walls to prevent erosion, and installing debris deflectors or catchers to reduce impact loads.[49,50] Where feasible, converting multi-span bridges to single-span bridges or adding relief openings can improve flow and reduce hydrodynamic forces on the piers. These measures directly target reducing the stress on structures during floods. While many post-flood investigations describe damage qualitatively, some have estimated the magnitude of the stress involved. In bridge steel components, 30 ksi can be a significant threshold corresponding to the early yield of standard structural steel and the fatigue limit for reinforcing bars.[51] Reports from flood failures often conclude that stresses surpassed this level. To be more specific, forensic analysis of a washed-out steel truss in Pennsylvania revealed flange stresses ranging from 22 to 30 ksi, due to debris loading high enough to cause plastic hinging in the connections.[52,53] In a case study, back-calculations of the collapsed concrete girder indicated that the internal steel reinforcement had yielded to 40 ksi when the span gave way.[54] During Typhoon Sinlaku, extreme flood discharge triggered rapid scour, undermining pier support. The forensic investigation reported flange stresses that were significantly above yield strength (36 ksi), resulting in plastic hinge formation and collapse of truss spans.[55] As noted, controlled experiments by TxDOT showed that at flow speeds roughly 1.5–2× the 100-year flood, bridge shear keys would experience shear stresses well above 20 ksi, indicating failure if no additional reinforcement is provided.[56]

In this study, to evaluate the flood-induced performance of bridge piers, stress values were recorded at nine incremental flood load levels ranging from 10 to 90 kip/in^2, representing the bridge pier response at each flood intensity. The resistance terms Performance-Level Resistance in Eq. (2) represent stress thresholds defining the boundaries between performance levels. These data points were then filtered based on defined stress thresholds to classify them into three performance zones: the IO performance zone (green) for stress levels below 20 kip/in^2, the material damage/LS zone (yellow) for stresses between 20 and 50 kip/in^2, and the CP state zone (red) for stresses exceeding 50 kip/in^2. For each zone, the whole dataset was filtered accordingly, and statistical parameters were computed. The mean stress value reflects the average structural response within a given performance category. At the same time, the standard deviation quantifies stress variability, indicating the consistency of the piers' performance under increasing flood loads. Fig. 1 depicts the schematic view of the flood loading distribution.

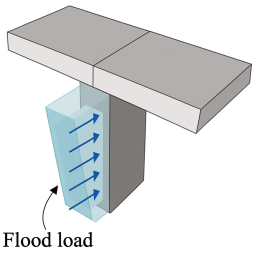

Figure 1. Schematic view of the flood-induced loading distribution

Following the statistical classification, the reliability of the bridge piers in each zone was assessed by calculating the probability of failure and the reliability index (β). Under the assumption that stress follows a normal distribution, the probability of failure was estimated as the area under the probability density curve beyond the defined failure threshold (50 kip/in^2), using the standard normal CDF. The reliability index β, which quantifies the safety margin, was computed as the standardized distance between the mean stress and the failure threshold, normalized by the standard deviation. A high β indicates acceptable reliability, while a low or negative β reflects inadequate performance or likely failure. This reliability-based methodology, combined with observations of flood-induced stress, supports a probabilistic framework for performance-based flood evaluation of bridge piers. It should be noted that flood IMs include peak flood loading to the deck elevation. The simulation data is used to estimate the probability of exceeding each

limit state. These exceedance probabilities are then fitted to a CDF, typically assumed to follow a lognormal distribution, to generate fragility curves for each damage state. Separate curves are developed for each pier configuration, allowing direct comparison of vulnerability based on pier diameter and design. These fragility curves provide a probabilistic representation of bridge system performance under uncertain flood loading, serving as foundational tools for resilience assessment, network-wide risk evaluation, and code calibration and performance-based design.

Following this, Fig. 2 illustrates the conceptual relationship between structural performance and increasing demand, highlighting three distinct damage states: IO, LS, and CP. These zones represent increasing levels of damage severity. In the immediate-occupancy zone, the bridge pier remains functional, with minimal damage and no significant loss of strength or serviceability. The LS zone indicates moderate degradation, characterized by cracking or localized material loss, where structural stability is maintained; however, repairs may be necessary. The CP zone corresponds to severe damage, including significant cracking or structural section failure, where the risk of collapse is high and the system can no longer ensure safety or operational capacity. The diagram also shows the global capacity curve, which captures the system's nonlinear response to escalating loading. As demands increase, such as from flood-induced forces, the structure transitions from elastic behavior toward progressive failure, aligning with the performance zones used in reliability and fragility assessments.

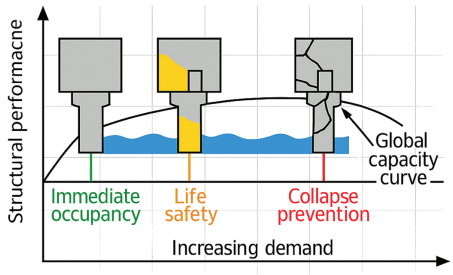

Figure 2. Qualitative performance levels subjected to the flood loading

Bridge structural models

In this study, a bridge model developed using SAP2000 for U.S. regional areas was adopted to represent a conventional highway bridge system. The structure consists of a steel girder superstructure and an RC substructure, with section properties and dimensions conforming to AASHTO-compliant standards. The girders have a cross-sectional area of approximately 10,776 in^2 with high flexural stiffness. The moment of inertia about the weak axis exceeds 1.47×10^8 in^4, indicating substantial lateral stiffness. The piers are modeled as square RC columns with equal moments of inertia (140,000 in^4) and a high torsional constant, providing good rotational resistance. The total height of the piers is 277 feet, with a depth of 36 feet and a width. Material properties and the bridge configuration model were summarized in Table 3 and Fig. 3.

Table 3. Material properties of the bridge model

Element	Material type	Specification	Modulus of elasticity (E)	Strength
Girders	Steel (pre-stressed)	AASHTO M270 Grade 50	~29,000 ksi	$Fy =$ 50 ksi
Piers	Reinforced concrete	AASHTO LRFD (normal weight)	~4,000 ksi	$f'c = 4$ ksi

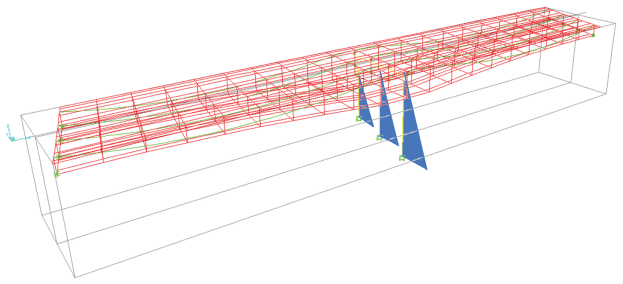

Figure 3. The steel girder bridge model layout under flood loading

Results and Discussion

The results presented in this section demonstrate a pioneering integration of nonlinear finite-element modeling, flood-specific hydrodynamic loading scenarios, and reliability-based performance evaluation to assess the vulnerability of bridge piers under extreme flood conditions. Unlike conventional design approaches, which largely overlook the probabilistic nature and localized effects of flood-induced stresses, this study employs a multistage modeling strategy that involves various nonlinear simulations to capture both the overall structural behavior and localized material damage. This hybrid global–local simulation approach, developed uniquely in this study, is further linked with probabilistic fragility and reliability assessments, enabling performance classification across IO, LS, and CP levels. By directly coupling realistic hydrodynamic loading conditions with material-level stress progression, the methodology offers a new pathway for flood-resilient bridge design, bridging the gap between deterministic structural evaluation and performance-based frameworks.

Finite-element flood simulations

One of the principal contributions of this study is the evaluation of bridge pier vulnerability under flood-induced stresses. While conventional bridge design standards primarily address gravity and traffic loads, they do not explicitly account for the structural impact of extreme hydrodynamic forces. This study aims to address this limitation by investigating damage propagation in reinforced concrete bridge

piers subjected to increasing flood stress levels. As mentioned in previous sections, an initial two-dimensional FEM analysis was conducted in SAP2000 to evaluate the global structural response of the bridge pier under flood-induced forces. This model captured the overall force–displacement behavior and identified critical stress regions. To achieve higher accuracy in capturing localized stresses, nonlinear material effects, and complex flood–structure interactions, a nonlinear FEM model was developed in ABAQUS. This model incorporated solid elements for the pier, explicit material constitutive laws, and realistic hydrodynamic loading distributions, enabling a more comprehensive assessment of pier performance and failure mechanisms. To estimate the critical limit states at which a column reaches damage, several nonlinear FEMs were developed and simulated using ABAQUS.[21] The columns were meshed with S4R elements, and the materials were selected from the default ABAQUS library. These simulations enabled detailed observation of stress development and damage accumulation in concrete and reinforcing steel elements. The stress responses captured in the analyses were used to assess the progression of structural degradation and to classify each configuration's performance. The resulting damage patterns and stress levels were categorized into three performance levels: IO, LS, and CP, based on established damage thresholds. As summarized in Table 4, increased flood loading scenarios resulted in more severe material responses and a gradual shift toward lower performance categories. The acquired observations confirm the pivotal role of hydrodynamic forces in structural vulnerability and highlight the importance of integrating flood-specific stress evaluations into performance-based bridge design frameworks.

Reliability assessment

Fragility analysis is performed based on the maximum stress values obtained from incremental flood-loading simulations. The results of this analysis are visualized using PDFs and normal probability plots, which assess the normality of stress distributions and illustrate the reliability characteristics of each performance zone.

The normal probability plots reveal distinct statistical behaviors across the three stress zones. In the Green (IO Zone), the data points lie close to the reference line with only minor tail deviations, indicating that the stresses reasonably follow a normal distribution and can be reliably modeled as such. In contrast, the Yellow (LS Zone) exhibits noticeable curvature and significant deviations at both tails, suggesting a skewed or mixed distribution resulting from the coexistence of relatively low stresses with higher values approaching or exceeding the failure threshold; this makes normal-based reliability estimates less representative for this range. As shown in Fig. 3, the Red (CP) aligns with the reference line in the mid-range. Still, it exhibits an upward deviation at the high end, indicating a heavy right tail where extreme stresses occur more frequently than expected under

Table 4. Performance levels of bridge piers subjected to flood loading with 20, 30, and 50 kip/in^2

Stress level	Severity	Damage state		Perf. level	Severity
		Concrete	Rebar		
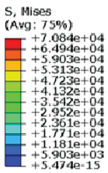	Low	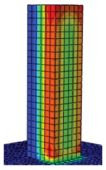	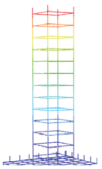	IO	
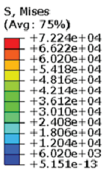	Moderate	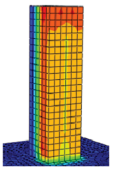	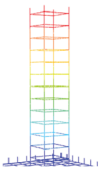	LS	
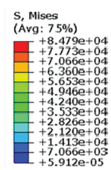	Elevated	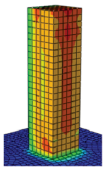	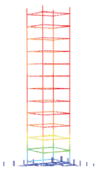	CP	
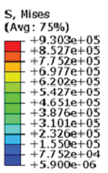	Extreme	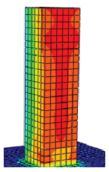	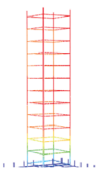	CP	

a purely regular model. Collectively, these patterns indicate that while the IO zone supports normal-based modeling, the LS zone may require fitting mixed or skewed distributions, and the collapse zone demands careful tail modeling to avoid underestimating the probability of extreme failure.

As shown in Fig. 4, in the LS zone (Yellow), the mean stress approaches the performance threshold, accompanied by significant variability. This combination increases the likelihood of failure and highlights potential structural vulnerabilities, indicating noticeable deviations in upper-tail values and risk concentrations. In the CP zone (Red), mean stress values exceed the failure threshold, resulting in a critically high probability of structural failure. This alarming situation requires urgent attention to enhance structural resilience. Fig. 5 illustrates the PDF of the CP zone, which exhibits a substantial deviation from normality, particularly at higher stress values.

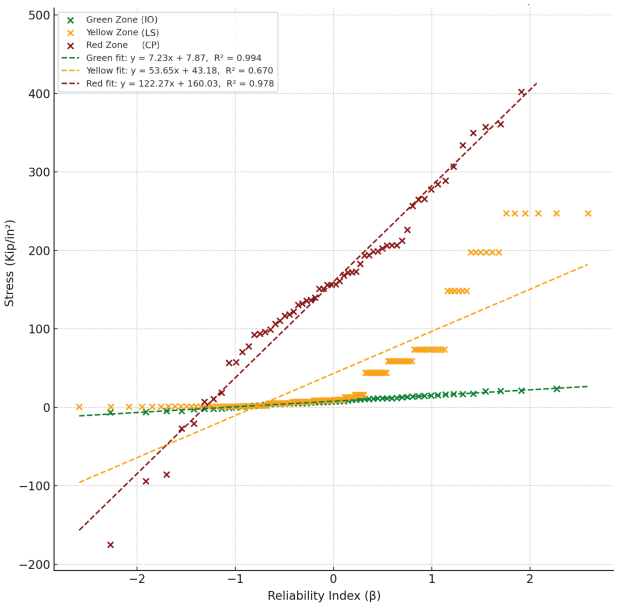

Figure 4. Normal probability plots for stress distributions in IO, LS, and CP performance zones under flood loading (representing the conditional probability of exceeding each performance threshold)

The reliability assessment clearly distinguishes between the three performance zones (Table 2). The serviceable zone exhibits strong structural integrity, with a reliability index of 2.7 and a failure probability of less than 0.004, which meets reliability expectations under moderate flood loading. The distress zone, while less severe than collapse, indicates potential material damage, with a low reliability index of 0.049 and nearly a 48% probability of exceeding the damage threshold. This marginal safety highlights a transitional state where strengthening may be needed. The CP zone, however, exhibits a concerning lack of reliability, with a failure probability above 80% and a reliability index of 0.862. These findings underscore the pressing need for design adjustments and reinforcement strategies to prevent catastrophic structural failure in future flood events. Based on the results,

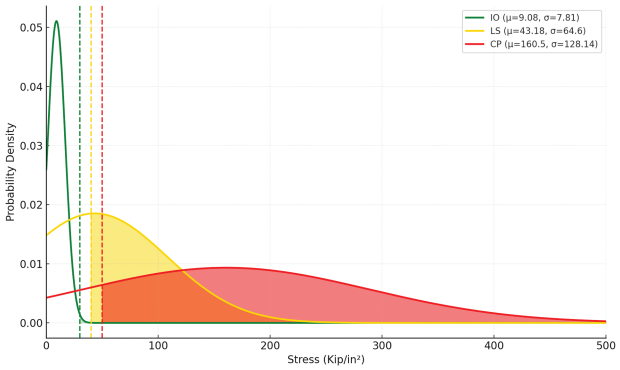

Figure 5. Probability density functions (PDFs) for bridge piers, considering three different performance levels, subjected to the flood loading

neither the distress nor the CP zones meet the target reliability thresholds set by design standards. Therefore, it is necessary to integrate reliability-based considerations into flood adaptation planning and prioritize structural upgrades in these zones. The failure probabilities (P_f) in Table 5 correspond to the fragility metrics defined in Section 2.2.2 and represent the conditional probability of exceeding each damage state under the applied flood loading. The increase from $P_f = 0.37\%$ for the IO state, 48% for LS, and 80.6% for CP reflect the rising vulnerability of the pier as flood intensity approaches or surpasses the associated performance limits. These probabilities, derived from the stress distributions shown in Figs. 4 and 5, provide the fragility characterization required for risk-informed bridge design.

Damage states and performance levels

Based on the observed results, the performance levels of the pier subjected to flood loading can be categorized by the damage states of its material. Various factors, including equilibrium equations, constitutive equations, and compatibility equations, influence the structural damage process. The equilibrium equation describes the internal stress distribution within the structure, while the compatibility equation defines the relationship between strain and deformation. To accurately estimate the structural response under flood-induced forces, a reliable constitutive model is needed to establish the relationship between stress and strain. The definition of damage depends on the material's constitutive behavior under hydrodynamic loading. The loading conditions, material properties, and the nonlinear response of structural components influence this behavior. In this study, several FEM analyses were conducted to investigate the progressive damage pattern of RC bridge piers subjected to flood loads.

Performance zones are defined according to stress thresholds obtained through incremental flood loading analyses. Table 6 outlines the performance-based visualization assessment for the FEM analysis interpretation.

As observed, the following performance classification can be applied to bridge pier performance under flood loading. The serviceable zone signifies conditions with acceptable

Table 5. Reliability outputs of the bridge pier subjected to the given flood loading

Zone	μ_{Q_F} (kip/in^2)	σ_{Q_F}	$\mu_{R_{PL}}$	P_f	β	Meets reliability?
IO	9.08	7.81	30	0.0037	2.679	Yes
LS	43.18	64.6	40	0.4804	0.049	No
Collapse prevention	160.5	128.14	50	0.8057	0.862	No

Table 6. Performance level of the pier based on observed structural conditions

Stress level	Concrete	Rebar	Piers performance
Low	Minor	Minor	Structure remains fully functional under flood conditions (IO)
Moderate	Minor	Significant	Structure may experience limited damage but remains stable (LS)
Elevated	Significant	Minor	Some cracking or yielding may occur; repairs may be needed (LS)
High	Significant	Significant	Structural safety is compromised; partial service disruption likely (LS)
Very High	Significant	Severe	Structure approaches failure limit; life safety concerns arise (CP)
Extreme	Severe	Significant	Structure is on the verge of failure; emergency intervention needed (CP)
Maximum	Severe	Severe	Structure likely to fail; complete loss of functionality expected (CP)

structural performance. The LS zone indicates moderate structural impairment that may necessitate remedial measures. The CP zone encompasses critical structural damage scenarios that require immediate attention to prevent catastrophic failure. The defined performance zones also integrate with established performance objectives: the serviceable zone corresponds to IO where the structure remains operational, the distress zone aligns with LS, allowing for limited damage without endangering users; and the CP zone reflects the CP objective, where failure is imminent unless emergency measures are performed.

Conclusions

This study presents a novel performance-based probabilistic framework for evaluating bridge pier vulnerability under flood loading, integrating hydrodynamic modeling, reliability analysis, and fragility assessment. Addressing critical gaps in current design standards, such as AASHTO LRFD, which lack explicit flood-specific load factors and performance criteria, the methodology incorporates flood intensity variability. It defines explicit stress-based damage states for bridge performance assessment. Through incremental flood loading analysis ranging from 10 to 90 kip/in^2 on representative U.S. highway bridge configurations, three stress-based performance thresholds were established and validated: IO at 20 ksi, LS at 40 ksi, and CP at 50 ksi. These thresholds were calibrated using forensic evidence from documented flood failures and extreme-event design guidelines, providing quantitative criteria currently absent from design codes.

Reliability assessment revealed stark differences across performance zones. The IO zone maintained adequate safety with a reliability index of 2.679 and a failure probability of 0.37 percent. However, the LS zone showed inadequate reliability, with an index of 0.049 and a failure probability of 48 percent, while the CP zone exhibited a negative reliability index of -0.862 and a failure probability of 80.6 percent. These results demonstrate that the LS and CP zones do not meet the target reliability thresholds of 3.0 or higher, indicating that current design practices that neglect flood-specific provisions significantly underestimate structural vulnerability. The framework demonstrates how reliability indices and failure probabilities combine to characterize flood vulnerability across intensity spectrums. The progression of failure probability from 0.37 percent to 80.6 percent quantifies the conditional probability of damage state exceedance, providing fragility metrics essential for probabilistic risk assessment. This integration captures both deterministic threshold behavior and probabilistic uncertainty in flood demands and structural capacity. Dynamic modeling revealed that flood-induced stresses can approach or exceed 50 ksi under extreme events with return periods

of 200 years or greater, triggering collapse mechanisms that current design practice does not explicitly account for in load combinations. This finding underscores the significant underestimation of vulnerability when flood loads are neglected in design evaluations.

This framework provides significant contributions toward future code development. The reliability indices enable calibration of flood load factors for load- and resistance-factor design-based approaches to achieve a target reliability of 3.0 or higher. The validated stress thresholds provide quantitative acceptance criteria for flood performance evaluation, enabling engineers to assess existing bridges and design new structures with explicit flood resilience objectives. Probabilistic failure metrics can be incorporated into transportation network resilience models to support system-level risk assessment and retrofit prioritization. Future research should extend this framework to diverse bridge configurations and geographical regions, incorporate climate change projections for nonstationary flood hazards, investigate multi-hazard scenarios combining flood with seismic or scour effects, and evaluate retrofit strategies. Additionally, integrating debris impact forces and foundation scour effects is necessary for a comprehensive flood vulnerability assessment. The urgent need for explicit integration of probabilistic flood assessments into bridge design standards is evident. Infrastructure resilience planning should prioritize the adoption of reliability-based methodologies and proactive retrofit measures, particularly for structures that exhibit inadequate performance in the LS and CP zones. Such approaches will significantly enhance the structural robustness and long-term resilience of transportation infrastructure facing escalating flood risks.

References

[1] Safari M, Ghasemi SH, Taghia SAHS, Norouzi Y. Integrating energy-based limit state functions to optimize target reliability of bridge pile for seismic events. *Transport Res Rec*. 2024;2678(2):863–875. doi:10.1177/03611981231176813.

[2] Hosseini P, Ghasemi SH, Jalayer M, Nowak SA. Performance-based reliability analysis of bridge pier subjected to vehicular collision: Extremity and failure. *Eng Fail Analy*. 2019;106(3):104176. doi:10.1016/j.engfailanal.2019.104176.

[3] Majtan E, Cunningham LS, Rogers BD. Flood-induced hydrodynamic and debris-impact forces on a single-span masonry arch bridge. *J Hydra Eng*. 2021;147(11):04021043. doi:10.1061/(asce)hy.1943-7900.0001932.

[4] Kabir SMI, Ahmari H, Dean M. Contribution of debris and substructures to hydrodynamic forces on bridges. *Eng Struct*. 2023;283:115878. doi:10.1016/j.engstruct.2023.115878.

[5] Kosič M, Anžlin A, Bau' V. Flood vulnerability study of a roadway bridge subjected to hydrodynamic actions, local scour and wood debris accumulation. *Water*. 2022;15(1):129. doi:10.3390/w15010129.

[6] Richardson EV, Davis SR. *Evaluating scour at bridges*. United States: Federal Highway Administration. Office of Bridge Technology; 2001.

[7] Anisha A, Jacob A, Davis R, Mangalathu S. Fragility functions for highway RC bridge under various flood scenarios. *Eng Struct*. 2022;260:114244. doi:10.1016/j.engstruct.2022.114244.

[8] Nasim M, Setunge S. Damage estimation of a concrete pier when exposed to extreme flood and debris loading. *J Marine Sci Eng*. 2022;10(5):710. doi:10.3390/jmse10050710.

[9] Xiong W, Cai CS, Zhang R, Shi H, Xu C. Review of hydraulic bridge failures: historical statistic analysis, failure modes, and prediction methods. *J Bridge Eng*. 2023;28(4):03123001. doi:10.1061/jbenf2.beeng-5763.

[10] Friedl C, Scheidl C, Wernhart S, Proske D. Assessing granular debris-flow impact forces on bridge superstructures. *J Bridge Eng*. 2024;29(6):04024027. doi:10.1061/jbenf2.beeng-6439.

[11] Zhang D, Xiong W, Ma X, Cai CS. Fragility evaluation of bridge pile foundation considering scour development under floods. *J Bridge Eng*. 2024;29(8):04024052. doi:10.1061/jbenf2.beeng-6665.

[12] Farrar CR, Worden K. An introduction to structural health monitoring. *Philosoph Transact Royal Soc A: Mathem, Phys Eng Sci*. 2007;365(1851):303–315. doi:10.1098/rsta.2006.1928.

[13] Ulfkjær JP, Krenk S, Brincker R. Analytical model for fictitious crack propagation in concrete beams. *J Eng Mech*. 1995;121(1):7–15. doi:10.1061/(asce)0733-9399(1995)121:1(7).

[14] Norouzi Y, Ghasemi SH. Probabilistic damage hazard analysis framework for crack detection by integrating Bayesian inference. *Eng Struct*. 2025;331:119939. doi:10.1016/j.engstruct.2025.119939.

[15] Rashid YR. Ultimate strength analysis of prestressed concrete pressure vessels. *Nucl Eng Des*. 1968;7(4):334–344. doi:10.1016/0029-5493(68)90066-6.

[16] Rabczuk T, Zi G, Bordas S, Nguyen-Xuan H. A simple and robust three-dimensional cracking-particle method without enrichment. *Comput Meth Appl Mech Eng*. 2010;199(37–40):2437–2455. doi:10.1016/j.cma.2010.03.031.

[17] Rabczuk T, Belytschko T. A three-dimensional large deformation meshfree method for arbitrary evolving cracks. *Comput Meth Appl Mech Eng*. 2007;196(29–30):2777–2799. doi:10.1016/j.cma.2006.06.020.

[18] Bažant ZP, Cedolin L. Blunt crack band propagation in finite element analysis. *J Eng Mech Div*. 1979;105(2):297–315. doi:10.1061/jmcea3.0002467.

[19] Jirasek M. *Modeling of Fracture and Damage in Quasibrittle Materials*. Doctoral dissertation. Northwestern University; ProQuest Dissertations and Theses Global; 1993. https://www.proquest.com/docview/304059266?pq-origsite=gscholar&fromopenview=true&sourcetype=Dissertations%20&%20Theses.

[20] Hillerborg A, Modéer M, Petersson P-E. Analysis of crack formation and crack growth in concrete by means of fracture mechanics and finite elements. *Cement Concr Res*. 1976;6(6):773–781. doi:10.1016/0008-8846(76)90007-7.

[21] Abaqus G. *Abaqus 6.11*, Dassault Systemes Simulia Corporation, Providence, RI, USA; 2011;3:73.

[22] Stephens JE, Yao JT. Damage assessment using response measurements. *J Struct Eng*. 1987;113(4):787–801. doi:10.1061/(asce)0733-9445(1987)113:4(787).

[23] Roufaiel MS, Meyer C. Reliability of concrete frames damaged by earthquakes. *J Struct Eng*. 1987;113(3):445–457. doi:10.1061/(asce)0733-9445(1987)113:3(445).

[24] Norouzi Y, Ghasemi SH, Nowak AS, Jalayer M, Mehta Y & Chmielewski J. Performance-based design of asphalt pavements concerning the reliability analysis. *Construct Build Mat*. 2022;332:127393. doi:10.1016/j.conbuildmat.2022.127393.

[25] Dong Y, Frangopol DM, Saydam D. Time-variant sustainability assessment of seismically vulnerable bridges subjected to multiple hazards. *Earthquake Eng Struct Dyn*. 2013;42(10):1451–1467. doi:10.1002/eqe.2281.
[26] Frangopol DM, Liu M. Maintenance and management of civil infrastructure based on condition, safety, optimization, and life-cycle cost. *Struct Infrastruct Syst*. 2019;96–108. doi:10.1080/15732470500253164.
[27] Biazar S, Kameshwar S, Balomenos GP. Multi-hazard fragility modeling framework for bridges with shallow foundations subjected to earthquake, scour, and vehicular loading. *Soil Dynam Earthq Eng*. 2024;178:108482. doi:10.1016/j.soildyn.2024.108482.
[28] Ellingwood BR. LRFD: implementing structural reliability in professional practice. *Eng Struct*. 2000;22(2):106–115. doi:10.1016/s0141-0296(98)00099-6.
[29] Frangopol DM, Ide Y, Spacone E, Iwaki I. A new look at reliability of reinforced concrete columns. *Struct Safety*. 1996;18(2–3):123–150. doi:10.1016/0167-4730(96)00015-x.
[30] Akgül F, Frangopol DM. Rating and reliability of existing bridges in a network. *J Bridge Eng*. 2003;8(6):383–393. doi:10.1061/(asce)1084-0702(2003)8:6(383).
[31] Nowak AS, Czernecki J, Zhou JH, Kayser JR. *Design loads for future bridges* (Report No. FHWA-RD-87-069). Springfield, VA, USA: National Technical Information Service; 1987.
[32] Nowak AS, Collins KR. *Reliability of Structures*. 2nd ed. CRC Press; 2012. doi:10.1201/b12913.
[33] Wu W, Tang S, Hou J, Li H, Elghazouli AY. Seismic performance of continuous rigid-frame bridges affected by flood-induced scour. *Structures*. 2025;71:107944. doi:10.1016/j.istruc.2024.107944.
[34] Habeeb B, Bastidas-Arteaga E. Assessment of the impact of climate change and flooding on bridges and surrounding area. *Front Built Environ*. 2023;9:1268304. doi:10.3389/fbuil.2023.1268304.
[35] Salvo G, Karakikes I, Papaioannou G, Polydoropoulou A, Sanfilippo L & Brignone A. Enhancing urban resilience: managing flood-induced disruptions in road networks. *Transport Res Interdiscip Perspect*. 2025;31(1–2):101383. doi:10.1016/j.trip.2025.101383.
[36] Dong S, Gao X, Mostafavi A, Gao J, Gangwal U. Characterizing resilience of flood-disrupted dynamic transportation network through the lens of link reliability and stability. *Reliab Eng Syst Saf*. 2023;232(1):109071. doi:10.1016/j.ress.2022.109071.
[37] Tubaldi E, White CJ, Patelli E, et al. Invited perspectives: challenges and future directions in improving bridge flood resilience. *Natural Haz Earth Syst Sci Discuss*. 2021;2021(3):1–21. doi:10.5194/nhess-22-795-2022.
[38] Li T, Lin J, Liu J. Time-varying seismic fragility analysis of bridges under the condition of the scour and freeze-thaw cycles. *European J Environ Civil Eng*. 2023;27(3):1179–1208. doi:10.1080/19648189.2022.2076746.
[39] Kameshwar S, Padgett JE. Multi-hazard risk assessment of highway bridges subjected to earthquake and hurricane hazards. *Eng Struct*. 2014;78:154–166. doi:10.1016/j.engstruct.2014.05.016.
[40] Ataei N, Padgett JE. Fragility surrogate models for coastal bridges in hurricane prone zones. *Eng Struct*. 2015;103(4):203–213. doi:10.1016/j.engstruct.2015.07.002.
[41] Norouzi Y, Ghasemi SH, Jalayer M. Probabilistic infrastructure failure cost analysis integrating with equity cost using the reliability analysis. *Computat Eng Phys Model*. 2025;8(2):19–45. doi:10.22115/cepm.2025.515772.1367.
[42] Bocchini P, Frangopol DM. A stochastic computational framework for the joint transportation network fragility analysis and traffic flow distribution under extreme events. *Probab Eng Mech*. 2011;26(2):182–193. doi:10.1016/j.probengmech.2010.11.007.
[43] Computers and Structures, Inc. *SAP2000® Integrated Structural Analysis and Design Software*. Berkeley, CA, USA; 1978.
[44] Pizarro A, Manfreda S, Tubaldi E. The science behind scour at bridge foundations: a review. *Water*. 2020;12(2):374. doi:10.3390/w12020374.
[45] Dorri F, Ghasemi SH, Jalilkhani M. Performance-based system reliability analysis for steel moment frames. *Structures*. 2023;51:472–483. doi:10.1016/j.istruc.2023.03.047.
[46] Shinozuka M. Development of bridge fragility curves based on damage data. *Earthquake Eng Engineer Seismol: Int J*. 2000;2(2):35–45.
[47] Kilgore R, Herrmann G, Thomas W, Thompson D. *HEC-17: highways in the river environment—floodplains, extreme events, risk, and resilience*. 2020.
[48] Arizona Department of Transportation (ADOT). *Highway Drainage Design Manual–Hydraulics*. Phoenix, AZ, USA.
[49] Lagasse PF, Zevenbergen LW, Schall JD, Clopper PE. *Bridge scour and stream instability countermeasures. experience, selection, and design guidance*. United States: Federal Highway Administration. Office of Bridge Technology; 2001.
[50] Bradley JB, Richards DL, Bahner C. *Debris Control Structures: Evaluation and Countermeasures*. Washington, DC, USA: US Department of Transportation, Federal Highway Administration; 2005.
[51] Roche JM, Klingner R, Fowler TJ. *Bridges with Premature Concrete Deterioration: Fatigue Testing of Full-Scale, Prestressed Concrete Box Girders Failing in Shear*. Austin, TX, USA: University of Texas at Austin; 2001.
[52] Wu T-R, Wang H, Ko Y-Y, et al. Forensic diagnosis on flood-induced bridge failure. II: Framework of quantitative assessment. *J Perform Construct Facilities*. 2014;28(1):85–95. doi:10.1061/(asce)cf.1943-5509.0000393.
[53] Ario I, Yamashita T, Tsubaki R, et al. Investigation of bridge collapse phenomena due to heavy rain floods: Structural, hydraulic, and hydrological analysis. *J Bridge Eng*. 2022;27(9):04022073. doi:10.1061/(asce)be.1943-5592.0001905.
[54] Pejović J, Serdar N, Pejović R. Damage assessment of road bridges caused by extreme streamflow in Montenegro: Reconstruction and structural upgrading. *Buildings*. 2022;12(6):810. doi:10.3390/buildings12060810.
[55] Hong J-H, Chiew Y-M, Lu J-Y, Lai J-S, Lin Y-B. Houfeng bridge failure in Taiwan. *J Hydr Eng*. 2012;138(2):186–198. doi:10.1061/(asce)hy.1943-7900.0000430.
[56] Ahmari H, Michelle H, Chiew Y-M, et al. *Identify and Analyze Inundated Bridge Superstructures in High Velocity Flood Events*. Arlington, TX, USA: University of Texas at Arlington; 2021.